JBC RESEARCH ARTICLE

The naturally occurring flavonoid nobiletin reverses methotrexate resistance *via* inhibition of P-glycoprotein synthesis

Received for publication, September 1, 2021, and in revised form, February 12, 2022 Published, Papers in Press, February 22, 2022,
https://doi.org/10.1016/j.jbc.2022.101756

Rui Liu[1], Yurong Song[1], Chenxi Li[1], Zhengjia Zhang[1], Zeyu Xue[1], Qingcai Huang[1], Liuchunyang Yu[1], Dongjie Zhu[1], Zhiwen Cao[1], Aiping Lu[2,*], Cheng Lu[3,*], and Yuanyan Liu[1,*]

From the [1]School of Chinese Materia Medica, Beijing University of Chinese Medicine, Beijing, China; [2]School of Chinese Medicine, Hong Kong Baptist University, Kowloon, Hongkong, China; [3]Institute of Basic Research in Clinical Medicine, China Academy of Chinese Medical Sciences, Beijing, China

Edited by Mike Shipston

Methotrexate (MTX) is the first-line treatment for rheumatoid arthritis (RA). However, after long-term treatment, some patients develop resistance. P-glycoprotein (P-gp), as an indispensable drug transporter, is essential for mediating this MTX resistance. In addition, nobiletin (NOB), a naturally occurring polymethoxylated flavonoid, has also been shown to reverse P-gp–mediated MTX resistance in RA groups; however, the precise role of NOB in this process is still unclear. Here, we administered MTX and NOB alone or in combination to collagen II-induced arthritic (CIA) mice and evaluated disease severity using the arthritis index, synovial histopathological changes, immunohistochemistry, and P-gp expression. In addition, we used conventional RNA-seq to identify targets and possible pathways through which NOB reverses MTX-induced drug resistance. We found that NOB in combination with MTX could enhance its performance in synovial tissue and decrease P-gp expression in CIA mice compared to MTX treatment alone. *In vitro*, in MTX-resistant fibroblast-like synoviocytes from CIA cells (CIA-FLS/MTX), we show that NOB treatment downregulated the PI3K/AKT/HIF-1α pathway, thereby reducing the synthesis of the P-gp protein. In addition, NOB significantly inhibited glycolysis and metabolic activity of CIA-FLS/MTX cells, which could reduce the production of ATP and block P-gp, ultimately decreasing the efflux of MTX and maintaining its anti-RA effects. In conclusion, this study shows that NOB overcomes MTX resistance in CIA-FLS/MTX cells through the PI3K/AKT/HIF-1α pathway, simultaneously influencing metabolic processes and inhibiting P-gp–induced drug efflux.

Rheumatoid arthritis (RA) is an autoimmune disease that is mainly characterized by erosive and symmetrical polyarthritis. The malignant proliferation of fibroblast-like synovial cells (FLS) of active RA plays a crucial role in the pathogenesis and progression of RA, including the formation of pannus, the secretion of proinflammatory cytokines, and cartilage degeneration (1). Methotrexate (MTX), the most common RA drug, has been widely used to treat RA since the 1980s (2). In addition, the use of MTX alone has been recommended for RA patients with low, medium, or high-risk disease activity (3). However, after taking MTX for a long time, it enters a plateau characterized by reduced multidrug sensitivity, thereby leading to poor curative effect, which ultimately results in multidrug resistance (MDR). Methotrexate-induced MDR is associated with several factors, among which the resistance of drug transporter-mediated MTX efflux in tumors is widely researched (4, 5). However, it has rarely been shown in RA.

The potential mechanism of MDR is intricate, with the ABC transmembrane protein, especially the MDR1 that encodes the transmembrane protein P-glycoprotein (P-gp), playing a crucial role (6). It is worth noting that MTX is one of a large number of substrates with binding sites on P-gp. Studies have revealed that P-gp mediates MTX-induced resistance which accounts for the therapeutic failure in RA (7, 8). Notably, the presence of P-gp can make cells more aggressive and/or easier to survive under adverse conditions. Similarly, ABC transporters have been studied for nearly 2 decades and found to be widely expressed in cell types associated with the pathogenesis of RA (9). Numerous studies have focused on P-gp as a prototype ABC transporter and have attempted to correlate P-gp expression with disease conditions and, more importantly, drug resistance (10). It has been reported that the level of P-gp is significantly higher in refractory RA patients than in non-refractory RA patients (11). All these findings suggest that P-gp–induced MTX efflux may be one of the indispensable causes of MTX resistance and desensitization in RA.

Nobiletin (NOB) is a naturally occurring flavone that is widely derived from the peel of citrus fruits and can be used as a chemical sensitizer (12). Studies have shown that the resistance of cancer cells to chemotherapy drugs, such as cisplatin, paclitaxel, and oxaliplatin, can be reduced by NOB (13). One study found that NOB inhibits P-gp activity, which paves the way for chemo-preventive agents to penetrate into cancer cells (14). In addition, NOB may target the PI3K-protein kinase B (AKT)/mTOR pathway to inhibit proliferation and growth of cancer cell, thereby exerting its antitumor activity (15).

* For correspondence: Yuanyan Liu, yyliu_1980@163.com; Cheng Lu, lv_cheng0816@163.com; Aiping Lu, lap64067611@126.com.

© 2022 THE AUTHORS. Published by Elsevier Inc on behalf of American Society for Biochemistry and Molecular Biology. This is an open access article under the CC BY-NC-ND license (http://creativecommons.org/licenses/by-nc-nd/4.0/).

Interestingly, our previous study found that combining the total flavonoid extract containing NOB and its derivatives with MTX may exert a synergistic effect for RA treatment (16), probably through inhibiting the proinflammatory cytokines and attenuating the development of RA (17). Therefore, this calls for studies to elucidate the potential mechanism of NOB in improving the sensitivity of CIA-FLS/MTX cells, with the overarching goal of providing insights into promoting the efficacy of RA treatment.

Fibroblast-like synovial cells interacts with B-cells and T-cells through hypoxia-inducible factor-1 α (HIF1-α) activation, thereby activating major signaling pathways (nuclear factor kappa beta, HIF1-α, and PI3K/AKT), which participate in various stages of RA development and increase glycolytic activity (18–20). For example, HIF1-α can affect energy supply and the level of lactic acid production, thereby participating in the invasion, migration, and survival of FLS cells (21, 22). Moreover, P-gp depends on the hydrolysis energy of ATP to excrete the drug out of the cells, and the concentration of MTX is always maintained at a low level in the cells (23). On the other hand, HIF-1α is a direct inducer of the expression of *MDR1* gene, which may physiologically upregulate P-gp. In this way, resistant cells possessed various armies, increased ATP supply, drug efflux pumps, and prosurvival pathways, which may be the integrally correlated causes of MTX resistance in RA. This study aimed at evaluating whether NOB can overcome MTX resistance in CIA-FLS/MTX cells by regulating P-gp and elucidating the mechanisms through which it targets different pathways to sensitize RA drug-resistant cells to chemotherapy.

Results

Arthritis index of collagen II-induced arthritis mice

The arthritis index (AI) results showed that the paw swelling and clinical manifestations of collagen II-induced arthritis (CIA) mice were higher than those of the normal group. At the same time, paw swelling was enhanced in the treatment group. Results indicated that the AI of mice in the NOB group was decreased compared to mice in the CIA group. Importantly, the combination of NOB and MTX significantly decreased the AI from day 46 compared to the AI of the MTX and NOB groups (Fig. 1*A*).

Effects of NOB on bone destruction in CIA mice

The protective effect of NOB and MTX alone or in combination on hind paws was measured using micro-CT. The bone surface/volume ratio of the NOB + MTX group decreased significantly compared to the CIA group. Interestingly, compared to the CIA group, the NOB group did not show effective bone protection (Fig. 1, *B* and *C*). These results suggest that the combination of NOB and MTX can effectively prevent bone destruction.

Nobiletin alleviates joint damage in CIA mice

To further explore the efficacy of NOB on CIA mice, the ankle joints of mice were subjected to histological analysis by H&E staining. Results showed that the joint structure of the sham operation group was complete, the cartilage surface was smooth, and there was no infiltration (Fig. 1, *D* and *E*). It was evident that NOB + MTX treatment significantly improved

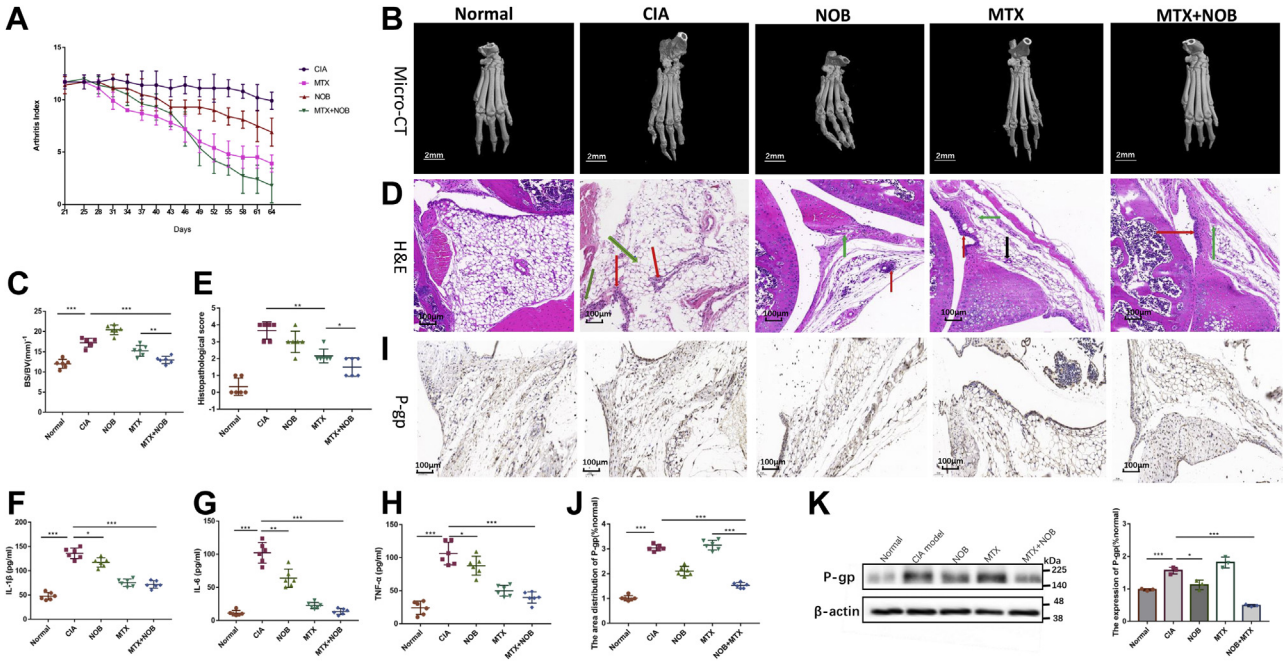

Figure 1. Effect of NOB on the arthritis severity in CIA mice and P-gp in synovial tissue. *A*, effect of NOB on the arthritis index. *B*, a microcomputer tomography image of the hind paw of a CIA mouse. *C*, bone surface/volume ratio (BS/BV; mm^{-1}). *D*, H&E staining of ankle joint tissue in each group. (The scale bar represents 100 μm) *Red arrow* indicates inflammatory cell infiltration; *green arrow* indicates disordered collagen fiber arrangement; and *black arrow* indicates artery. *E*, histological score of each group. *F–H*, levels of IL-1β, IL-6, and TNF-α in mice ankle tissue. *I*, immunohistochemistry results about P-gp (the scale bar represents 100 μm). *J*, the area distribution of P-gp. *K*, Western blot results. CIA, collagen II-induced arthritis; IL, interleukin; NOB, nobiletin; P-gp, P-glycoprotein. $*p < 0.05$, $**p < 0.01$, $***p < 0.001$.

synovial hyperplasia and decreased the severity of cartilage damage and inflammatory cell infiltration.

Inflammatory cytokines of CIA mice

Enzyme-linked immunosorbent assay results showed that the CIA group had higher levels of tumor necrosis factor-alpha (TNF-α), interleukin-6 (IL-6), and interleukin-1β (IL-1β) compared to the normal group (Fig. 1, *F–H*). Both the MTX and NOB groups could reduce the content of TNF-α, IL-6, and IL-1β in the ankle joint. Moreover, the levels of TNF-α, IL-6, and IL-1β in the NOB + MTX group were closer to normal levels compared to the single treatment groups. These results suggest that the combined treatment of NOB and MTX exhibits a stronger inhibitory effect on inflammatory cytokines.

Effect of NOB on the expression of P-gp in the synovial tissue of CIA mice

Figure 1*K* shows that the P-gp expression of the CIA group was significantly higher than in the normal group. P-glycoprotein expression was significantly downregulated in the NOB group compared to the CIA group. Immunohistochemistry results (Fig. 1, *I* and *J*) also showed that the P-gp expression was higher in the MTX group than in the normal group after treatment. However, the P-gp expression was downregulated after treating with MTX and NOB combined (Fig. 1*K*). These results indicated that NOB treatment could reverse the MTX resistance of CIA mice in the synovial tissue through reducing the expression of P-gp. Given that P-gp is closely associated with drug resistance, it is indispensable to explore the potential mechanism of NOB in drug resistance.

Nobiletin overcomes MTX resistance in CIA-FLS/MTX cells

Cell counting kit-8 assay was performed to confirm whether CIA-FLS/MTX cells are indeed resistant to MTX. Results indicated that MTX (0–50 μg/ml) significantly decreased cell viability in fibroblast-like synoviocytes from collagen-induced arthritis (CIA-FLS) parental cells in a time- and dose-dependent manner but showed little cytotoxicity against CIA-FLS/MTX cells (Fig. 2, *D–F*). Cell counting kit-8 assay results showed that the viability of CIA-FLS cells was influenced by high doses of NOB (>100 μM) (Fig. 2, *A–C*). Therefore, NOB at a concentration of 80 μM was used as the optimum dose in the subsequent experiments.

To evaluate whether the combination of NOB and MTX can synergistically kill CIA-FLS/MTX cells, CIA-FLS/MTX cells were treated with increasing concentrations of NOB and MTX, either alone or in combination, for 48 h. Figure 2*E* shows that the addition of NOB significantly sensitized

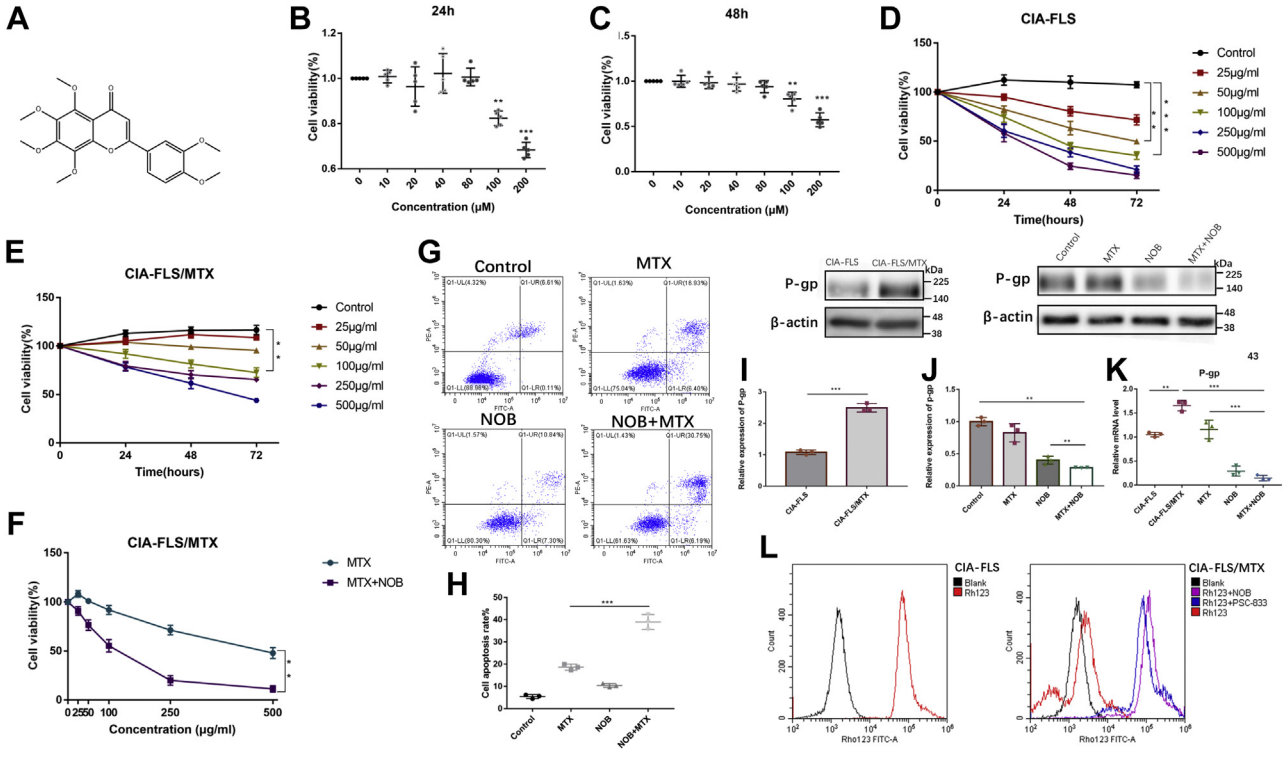

Figure 2. The chemical effect of NOB on CIA-FLS viability and cytotoxic effects, expression and activity of P-gp, and apoptosis of NOB and MTX in two cell lines. *A*, the chemical structure of NOB. The cells are cultivated with increasing concentrations of NOB (0, 10, 20, 40, 80, and 100 μM) for 24 h (*B*) and 48 h (*C*). Methotrexate (25, 50, 100, 250, and 500 μg/ml) efficiently decreased the viability of CIA-FLS cells (*D*) and CIA-FLS/MTX cells (*E*) at 24, 48, and 72 h. *F*, the combination of NOB and MTX synergistically decreased the viability of CIA-FLS/MTX cells at 72 h. The cell viability was measured by CCK-8 assay. *G*, MTX (100 μg/ml), NOB (80 μM), and the combination of NOB with MTX treatment (24 h) induced apoptosis in CIA-FLS/MTX cells. Apoptosis was measured by Annexin V/PI staining and flow cytometry ($p < 0.05$). *H*, the quantitative results of apoptosis rate. *I*, the expression of P-gp in CIA-FLS and CIA-FLS/MTX cells. *J*, Western blot results. Nobiletin (80 μM), MTX (100 μg/ml), or their combination affected P-gp expression in CIA-FLS/MTX cells. *K*, RT-qPCR results. *L*, the effect of NOB on P-gp substrate efflux activity was assessed. CIA, collagen II-induced arthritis; CCK-8, cell counting kit-8; FLS, fibroblast-like synovial cells; MTX, methotrexate; NOB, nobiletin; P-gp, P-glycoprotein; RT-qPCR, quantitative reverse-transcription PCR. $^{**}p < 0.01$, $^{***}p < 0.001$.

CIA-FLS/MTX cells to MTX. Notably, the combined treatment exhibited a synergistic inhibitory effect in CIA-FLS/MTX cells (Table 1). Altogether, these results suggest that the combination of NOB and MTX has an inhibitory effect on drug-resistant cells.

Nobiletin induces apoptosis in CIA-FLS/MTX

Flow cytometry was used to explore the effect of NOB on drug-induced apoptosis in CIA-FLS/MTX-resistant cells. Briefly, CIA-FLS/MTX cells were treated with NOB and MTX, either alone or in combination, for 24 h, followed by measuring the apoptosis rate using Annexin V/PI analysis. The results indicated that the apoptosis rate of the NOB + MTX group was significantly higher than that of the CIA-FLS/MTX group and MTX group (Fig. 2, *G* and *H*). These findings suggest that NOB could increase the apoptosis rate of MTX-resistant CIA-FLS/MTX cells.

Effects of NOB on P-gp function and expression

Studies have shown that NOB and its derivatives sensitize drug-resistant cells to different pathways. Considering that NOB can increase the apoptosis of CIA-FLS/MTX cells, we explored whether NOB could inhibit resistance of RA by downregulating P-gp expression. To verify this hypothesis, Western blot and quantitative reverse-transcription PCR were performed to measure the level of P-gp. Results showed that P-gp was more expressed in CIA-FLS/MTX cells than in CIA-FLS cells (Fig. 2*I*). We further explored whether NOB affects the expression and function of P-gp (Fig. 2*J*). The results revealed that using NOB or MTX alone or in combination would significantly reduce the mRNA level of P-gp in CIA-FLS/MTX cells (Fig. 2*K*). Rh123, which is a known substrate of P-gp, is commonly used to monitor the function of P-gp. Results obtained in this study showed that Rh123 accumulated in CIA-FLS cells, but not in CIA-FLS/MTX cells (Fig. 2*L*). Notably, NOB particularly promoted the entry of Rh123 into CIA-FLS/MTX cells. These results suggest that NOB paved the way for the penetration of MTX into CIA-FLS/MTX cells by partially inhibiting the activity and function of P-gp.

RNA-sequencing analysis

RNA-seq transcriptome analysis was conducted for in-depth discovery of potential molecular targets and related pathways of NOB. In addition, gene enrichment analysis further revealed the molecular function of differentially expressed genes (DEGs) and their associated biological pathways. Interestingly, a comparison between the MTX group and the control group found 10,929 DEGs, among which 5825 were upregulated and 5104 were downregulated (Fig. 3*A*). Besides, there were 7509 DEGs between the NOB + MTX group and the MTX group, of which 3890 were upregulated and 3619 were downregulated (Fig. 3*B*). In addition, cluster analysis showed that the DEGs in each group were uniform (Fig. 3*C*).

Gene ontology analysis mainly analyzes the biological processes, molecular functions, and cellular components of DEGs. Herein, gene ontology enrichment analysis between the MTX group and the NOB + MTX group indicated that the DEGs were mainly associated with metabolic processes (Fig. 3*D*). The molecular function of the DEGs was mainly associated with the activity of protein bands. Moreover, Kyoto Encyclopedia of Genes and Genomes pathway analysis found 20 pathways closely associated with the DEGs, including metabolism, HIF-1 signaling, and glycolysis/gluconeogenesis pathways (Fig. 3*E*). Combining our RNA sequence analysis results and the findings of previous studies (21, 24), we can speculate that HIF-1 and metabolic signal transduction pathways are the main pathways through which NOB performs its functions.

Table 1
IC 50 value of methotrexate and Nobiletin in cells

Drug	IC50 ± SD(μg/ml)		RI
	CIA-FLS/MTX	CIA-FLS	
MTX	354.30 ± 11.30[a]	46.99±2.47	7.54
MTX(μg/ml)+NOB	121.01 ± 5.35[a]	10.28±0.35	11.77

[a] $p < 0.001$, compared to CIA-FLS cells. IC50: half maximal inhibitory concentration; RA: rheumatoid arthritis; MTX: methotrexate; NOB: nobiletin; RI: resistance index; CIA-FLS: fibroblast-like synoviocytes from collagen-induced arthritis; CIA-FLS/MTX: MTX-resistant fibroblast-like synoviocytes from collagen-induced arthritis.

Nobiletin activates the PI3K/AKT/HIF-1 signaling pathway in vitro

To verify the RNA-seq results, we further analyzed the HIF-1 signaling pathway where we measured the level of HIF-1α, a key protein in the HIF-1 signaling pathway. Quantitative reverse-transcription PCR was used to determine the mRNA level of HIF-1α (Fig. 4*E*), with obtained results indicating that the RNA-seq method was accessible. Next, the levels of PI3K and AKT, independent proteins that interact with HIF-1α upstream of the HIF-1 signaling pathway, were also evaluated. In addition, we evaluated the effect of NOB on the PI3K/AKT/HIF-1α signaling pathway. Results showed that the expression of HIF-1α and phosphorylated AKT were significantly decreased in the NOB + MTX group compared to the MTX group, but PI3K and total AKT protein levels were not affected (Fig. 4, *A*–*D*). This result suggests that NOB might downregulate the PI3K/AKT/HIF-1 signaling pathway.

Nobiletin reduces glycolysis and energy supply in CIA-FLS/MTX cells

Fibroblast-like synoviocytes from collagen-induced arthritis in synovial tissues are more inclined to use the glycolytic pathway, whereas resting cells commonly use the oxidative phosphorylation pathway. Likewise, a previous study found that glucose metabolism is increased in CIA-FLS cells (24). Interestingly, RNA-seq analysis showed that NOB treatment significantly downregulated metabolism and glycolysis signaling pathways in CIA-FLS/MTX cells. Subsequently, we assessed whether MTX resistance would alter the metabolism of CIA-FLS/MTX cells and observed the production of ATP and lactic acid. The results showed a significant increase in

ASBMB

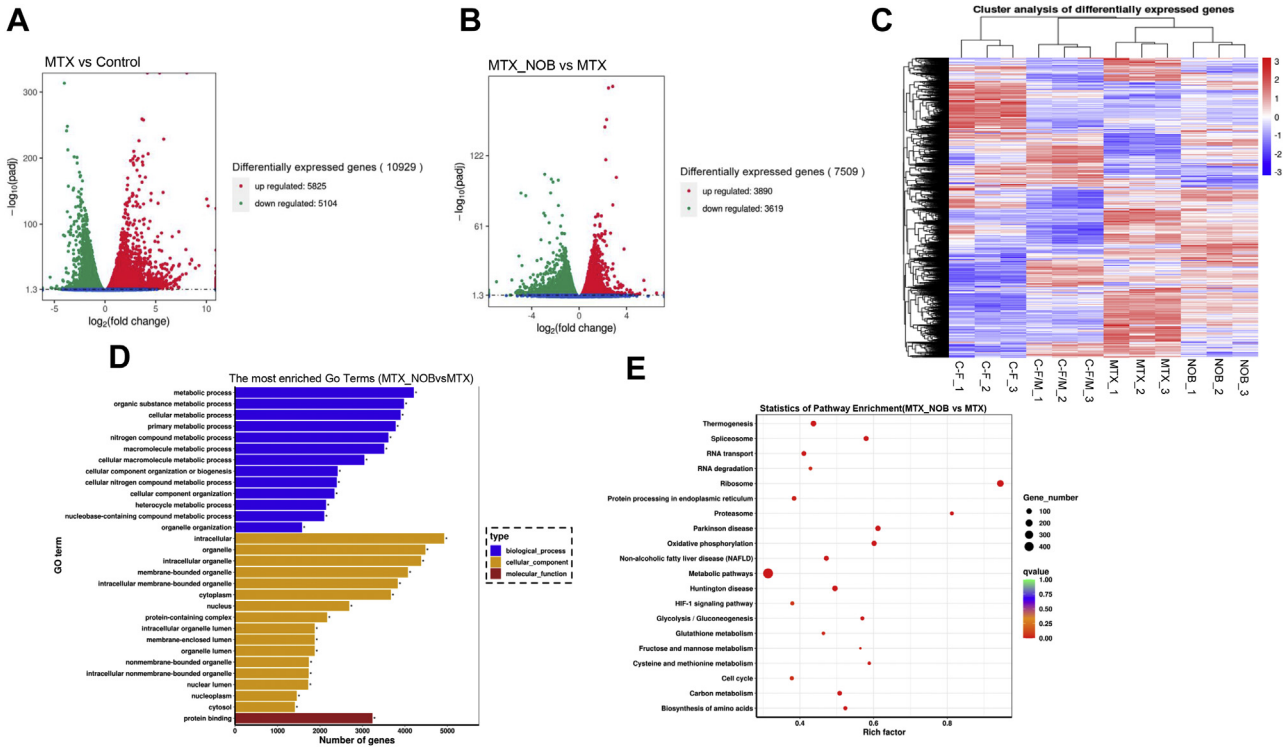

Figure 3. RNA-seq results. *A* and *B*, the DEGs consequence. *C*, cluster analysis of DEGs. *D*, gene ontology enrichment analysis. *E*, Kyoto Encyclopedia of Genes and Genomes analysis. DEGs, differentially expressed genes.

glucose consumption in CIA-FLS/MTX cells compared to CIA-FLS cells. We also found a significant decrease in cellular ATP levels, glucose consumption, and lactate production in the NOB + MTX group (Fig. 5, *A–C*). Next, the effect of NOB on improving glycolysis rate in CIA-FLS/MTX cells against MTX was evaluated. Previous studies have shown that the microenvironment caused by arthritis could lead to the upregulation of *GLUT-1* in FLS. On the other hand, hexokinase-II (HK-II) plays a vital role in the conversion of glucose into subsequent products and the increase of cellular metabolic activity. In this study, these genes were observed in CIA-FLS/MTX cells, with results showing that their levels

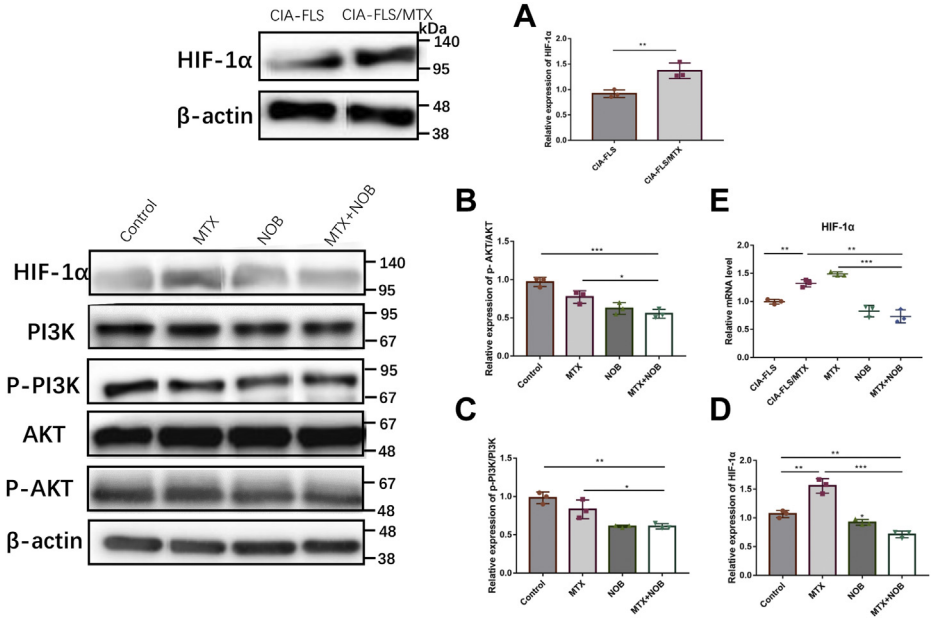

Figure 4. Effects of NOB on the AKT/HIF-1α signaling pathway in CIA-FLS/MTX cells. *A*, hypoxia-inducible factor-1 α expression in CIA-FLS and CIA-FLS/MTX cells. *B-D*, the relative expression of AKT, PI3K, and HIF-1α in different groups. *E*, quantitative reverse-transcription PCR results of HIF-1α. NOB, nobiletin; CIA, collagen II-induced arthritis; AKT, protein kinase B; FLS, fibroblast-like synovial cells; HIF1-α, hypoxia-inducible factor-1 α; MTX, methotrexate. *$p < 0.05$, **$p < 0.01$, ***$p < 0.001$.

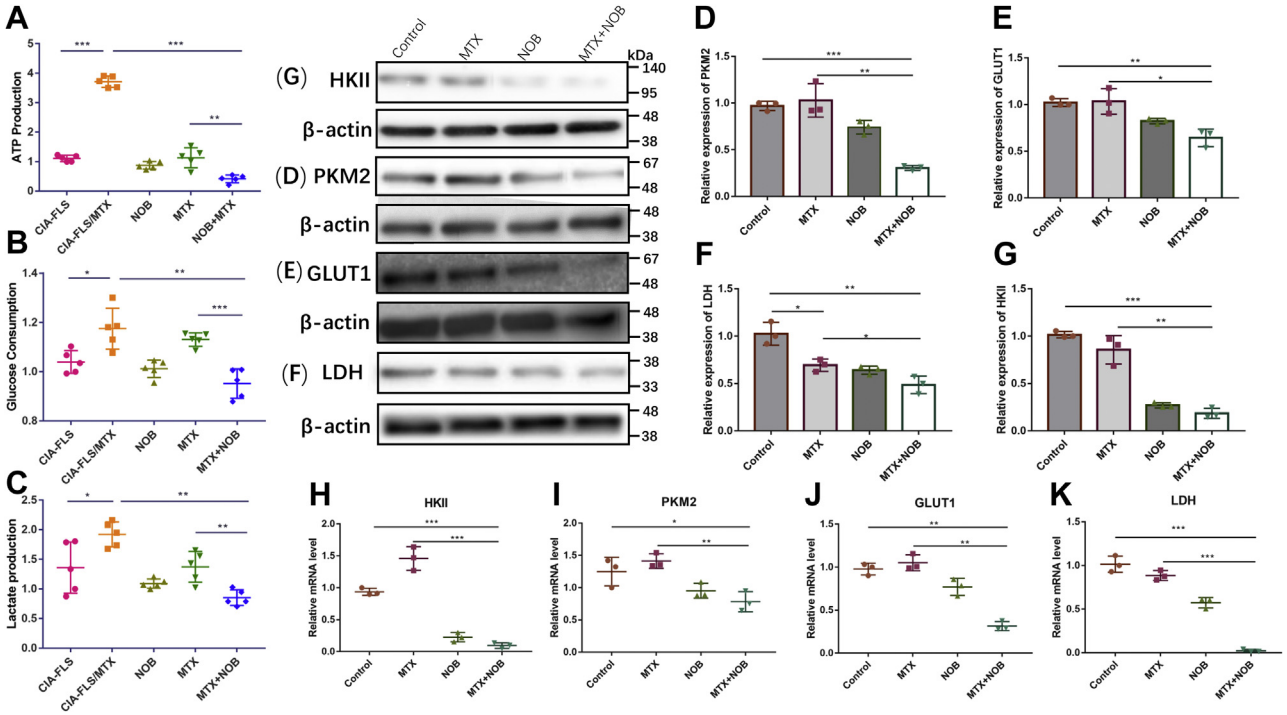

Figure 5. The effect of NOB on glycolysis status in CIA-FLS/MTX cells. *A*, ATP production. *B*, glucose consumption. *C*, lactate export. Western blot images of (*D*) PKM2, (*E*) GLUT1, (*F*) LDH, and (*G*) HK-II protein expression levels. *H–K*, quantitative reverse-transcription PCR results. CIA, collagen II-induced arthritis; FLS, fibroblast-like synovial cells; GLUT1, glucose transporter 1; HK-II, hexokinase-II; LDH, lactate dehydrogenase; MTX, methotrexate; NOB, nobiletin; PKM2, pyruvate kinase isozyme type M2.

were significantly decreased after NOB treatment (Fig. 5, *D–K*). These results suggest that NOB might reduce glucose metabolism and glycolysis and may reverse the drug resistance of CIA-FLS/MTX cells.

Knockdown of AKT1 or HIF-1α can enhance the NOB-induced reduction of P-gp in CIA-FLS/MTX cells

To confirm that NOB reverses RA resistance through the AKT/HIF-1α pathway, *AKT* and *HIF-1α* knockdown was performed in CIA-FLS/MTX cells using specific siRNAs. Western blotting was performed on cells transfected with siAKT family to confirm successful silencing (Figure SA-B). Finally, AKT and HIF-1α were inhibited in CIA-FLS/MTX cells using siAKT1 and siHIF-1α (specific siRNAs). Notably, the control group was transfected with scrambled siRNA (siControl). After 48 h, Western blot analysis was performed to evaluate the knockdown effect of specific siRNA. Results showed that the specific siRNA could significantly inhibit the expression of AKT1 and HIF-1α in the experimental group (Fig. 6, *A–C*). Moreover, the expression of HIF-1α was downregulated in the siAKT1 treatment group, but there was no significant change in the expression of AKT1 in the siHIF-1α treatment group (Fig. 6, *D* and *E*). This implies that HIF-1α is a downstream effector protein of the AKT signal transduction pathway and is regulated by AKT. Meanwhile, the level of P-gp was carefully measured. Results showed that the downregulation of P-gp expression was enhanced by NOB in CIA-FLS/MTX cells transfected with siAKT1 and siHIF-1α (Fig. 6, *F–H*). Collectively, these findings further confirm that NOB downregulates P-gp expression through the PI3K/AKT/HIF-α signaling pathway.

Discussion

Although the pleiotropic effects of NOB have been well described in previous studies (13), the exact mechanism through which NOB reverses RA resistance in drug-resistant cells has not yet been fully elucidated. Notably, understanding these events may help reverse and treat RA. Herein, we established a CIA mice model and used it to study the effect of NOB and MTX treatment on P-gp expression in RA. It was found that the combined treatment of NOB and MTX significantly downregulated the expression of P-gp compared to the MTX group. Results also indicated that NOB combined with MTX could reduce cartilage and bone damage *in vivo* and improve paw swelling and arthritis damage in CIA mice. Interestingly, AI and micro-computed tomography (CT) results revealed that NOB could slightly reduce AI probably through reducing the inflammation, but it had no effect on bone destruction. However, NOB combined with MTX could exert a significant decrease in AI and bone destruction compared to CIA and MTX group, which suggests that NOB might synergize with MTX through reversing MTX-induced drug resistance. Moreover, the results indicated that P-gp could be downregulated by NOB in RA, thereby reducing the outflow of MTX and maintaining the effect of MTX. To further prove this phenomenon, MTX-resistant CIA-FLS/MTX cells were used to explore whether NOB could make MTX sensitive to MDR in CIA-FLS cells.

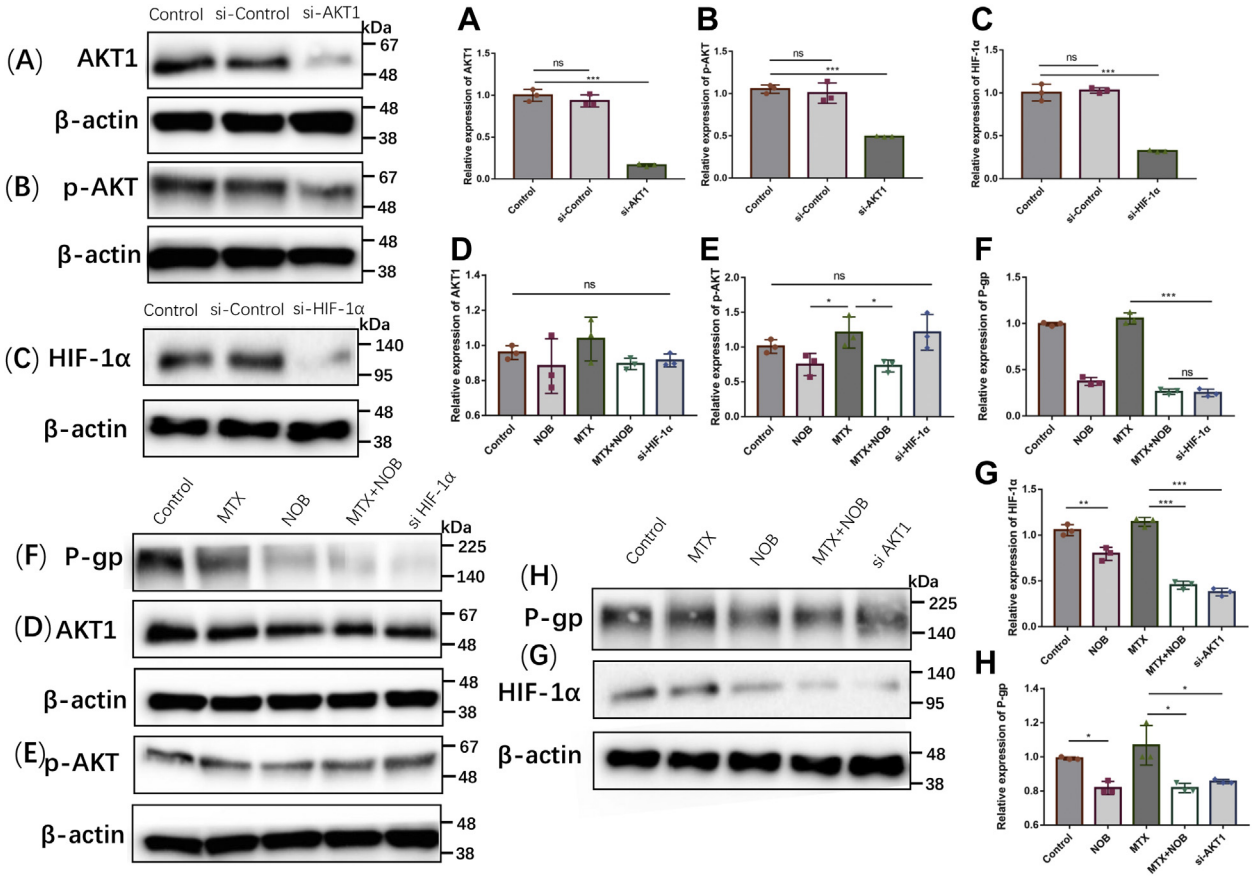

Figure 6. Effects of siRNA transfection on the AKT/HIF-1α signaling pathway and the expression of P-gp. *A–C*, knockdown efficacy of *AKT* and *HIF-1α*. *D–H*, relative expression *of AKT, p-AKT, HIF-1α*, and *P-gp* in different groups. AKT, protein kinase B; HIF1-α, hypoxia-inducible factor-1 α; P-gp, P-glycoprotein.

Significant synergy was observed between NOB and MTX in CIA-FLS/MTX cells. Notably, NOB (at noncytotoxic concentrations) + MTX cotreatment resulted in the restoration of growth inhibition and apoptosis of CIA-FLS/MTX cells. Flow cytometry analysis demonstrated that NOB could accelerate MTX-mediated apoptosis of CIA-FLS/MTX cells, suggesting that NOB might serve as a chemosensitizer to overcome drug resistance in RA.

It has been reported that one of the crucial causes of MDR in cancer is P-gp–mediated efflux transportation of chemotherapeutic drugs (25). In this study, P-gp was highly expressed in drug-resistant CIA-FLS/MTX cells. Therefore, we further explored the role of NOB in regulating the function and expression of P-gp and increasing the efficiency of MTX. Results showed that, in the presence of NOB, P-gp was inhibited in CIA-FLS/MTX cells, whereas uptake of Rh123 (a P-gp substrate) was increased, further demonstrating NOB-mediated P-gp inhibition. These results suggest that NOB might regulate the function and the level of P-gp in RA, thereby reducing the outflow of MTX and maintaining the effect of MTX.

RNA-sequencing as a common genome analysis technology that can be used to identify molecular targets and related pathways for drug discovery (26). Herein, RNA-seq was used to reveal the potential mechanism through which NOB acts as a chemosensitizer to overcome MDR in RA. Results indicated that the HIF-1 signaling pathway was significantly downregulated by NOB treatment. Correspondingly, the Kyoto Encyclopedia of Genes and Genomes map further revealed that HIF-1α, a key protein in the HIF-1 signaling pathway, was also downregulated. Activation of the HIF-1 signaling pathway may stimulate the synovium and maintain the chronic, self-sustaining, and continuous infiltration of immune cells, which leads to the phenotypic change of CIA-FLS and the invasion of adjacent cartilage (27). Similarly, the PI3K/AKT pathway is widely distributed in synovial tissues, involved in the proliferation, apoptosis, and migration of FLS, and the formation of vasospasm (28). Given that HIF-1α, a direct inducer of *MDR1* gene expression, is regulated by the upstream pathway of PI3K/AKT, it can physiologically upregulate P-gp (29, 30). Therefore, this study explored the expression of PI3K, AKT, and HIF-1α under varied conditions. Results showed that, under normal oxygen levels, there was a difference in the expression level of HIF-1α between CIA-FLS and CIA-FLS/MTX cells. Meanwhile, it was found that NOB treatment significantly reduced the levels of p-AKT and HIF-1α in CIA-FLS/MTX cells compared to the control group. However, there was no significant change in the total AKT and PI3K. Therefore, we speculated that the change in AKT in this study might be due to the direct effect of NOB on

phosphorylated AKT instead of PI3K, which needs to be verified in future studies. These findings partially emphasized the usefulness of RNA-seq in revealing PI3K/AKT/HIF-1α as the intrinsic molecular pathways of NOB intervention.

In the early stage of RA, glucose metabolism is significantly increased in the joints of RA patients. The activation of FLS and subsequent joint damage is associated with metabolic changes, especially glucose metabolism. It has been reported that increased glucose metabolism is induced by the main pathways associated with cell survival, angiogenesis, and invasion of FLS cells (31). The increased glucose consumption and lactate output indicated that MTX-resistant CIA-FLS/MTX cell lines exhibited an enhanced metabolic phenotype compared to MTX-sensitive CIA-FLS cells. This is because the metabolic changes can endow CIA-FLS/MTX cells with the advantages of adaptability, proliferation, survival, and drug resistance. In addition, RNA-seq analysis showed that NOB treatment significantly downregulated metabolism and glycolysis signaling pathways. Furthermore, we assessed the expression of glucose metabolism under varied conditions, with obtained results indicating that cellular ATP levels, glucose consumption, and lactate production were significantly reduced after NOB treatment. The detection of key glycolytic proteins showed that the NOB + MTX group significantly reduced the expression levels of HK-II and glucose transporter 1 (GLUT1) and the activities of lactic dehydrogenase (LDH) and pyruvate kinase isozyme type M2 (PKM2) compared to CIA-FLS/MTX cells. These results suggest that drug resistance might require more glycolytic metabolism adaptability, which could modulate the MDR phenotype of CIA-FLS/MTX cells. Nobiletin treatment could downregulate this metabolic process of pump function for energy and nutrition supply. It is worth mentioning that enhanced glycolysis has been shown to produce a sea of intermediate metabolites, including proteins, lipids, and nucleotides, which could support the synthesis of macromolecules needed for cell proliferation (32). Furthermore, the increase in aerobic glycolysis leads to a concomitant increase in lactic acid production, which can lessen the absorption and efficiency of the drug by upregulating the H^+-linked ATPase and transporter (33). The results of this study suggest that the rapid ATP supply in CIA-FLS/MTX cells might activate P-gp through glycolysis and maintaining drug efflux, whereas NOB could inhibit glycolysis, consume ATP, and block P-gp.

A previous study reported that intracellular sensors are activated under some stressful conditions, including chemotherapy or hypoxia, and PI3K/Akt and sirtuins-dependent axis, as well as downstream transcription factors (nuclear factor-kB, Nrf2, and HIF-1α) can enhance stress resistance (30). Majority of these converters and transcription factors may activate the survival and proliferation pathways, especially for the induction of ABC transporters. Parallel to these consequences, these pathways also induce massive reprogramming of cellular energy/metabolic functions through glycolytic HIF-1α and PI3K/AKT axes and has a significant outcome on HK-II, PKM2, and LDH expression. To further verify the role of the PI3K/AKT/HIF-1 signaling pathway in regulating CIA-FLS/MTX resistance, two highly specific siRNAs were used to specifically knockdown the expression of *AKT1* and *HIF-1α*. The results showed that P-gp expression was downregulated after *AKT1* and *HIF-1α* knockdown. Collectively, the findings of this study have shown that NOB can regulate the PI3K/AKT/HIF-1α signaling pathway, reduce the expression of P-gp, and downregulate the expression of glycolysis to a certain extent.

Conclusion

This study found that NOB could reverse the MTX-induced MDR in CIA-FLS/MTX cells at noncytotoxic concentrations. The synergistic effect between MTX and NOB may be partially associated with P-gp–mediated MDR and the glycolysis pathway. In particular, NOB downregulated the PI3K/AKT/HIF-1α signaling pathway, thereby reducing the production of downstream P-gp protein, inhibiting drug transporter–mediated MTX efflux, and maintaining the therapeutic efficacy. Similarly, NOB significantly inhibits glycolysis and metabolic activity of CIA-FLS/MTX cells for energy and nutrition supply, which may result in enhanced fragility of cells, thereby increasing sensitivity of the response to MTX (Fig. 7). Our findings provide new insights and corresponding verification for using NOB as a chemosensitizer on RA in overcoming MTX-induced MDR. Future studies can use the MTX-resistant RA model established in this study to explore the effect of NOB on drug resistance in tumors and elucidate the exact mechanism through which NOB regulates adaptive glucose changes in drug-resistant cells.

Experimental procedures

Chemicals and reagents

Nobiletin (CAS: 478013, purity >98%) was obtained from Shanghai Source Leaf Biological Technology, whereas MTX (purity >99%) was supplied by Toronto Research Chemicals Inc. PSC-833 was obtained from MedChemExpress. Rhodamine 123 (Rh123) was purchased from Fluorescence. Glucose, lactate, and ATP assay kits were bought from Jiancheng Bioengineering Institute. Short interfering RNA, including AKT1, HIF-1α, and negative control siRNA, were obtained from Fenghui Biology. Fetal bovine serum (FBS) and TRIzol reagent (15596026) were purchased from Thermo Fisher Scientific. Anti-P-gp (ab170904), AKT (4691T), AKT1(75692S), p-AKT (4060T), PI3K (4257T), p-PI3K (17366S), PKM2 (4053T), HK2 (2867T), LDHA (2012S), GLUT1 (12939S), HIF-1α (14179S), and β-actin (4970T) antibodies were purchased from Abcam or Cell Signaling Technology.

Establishment of CIA model

Male DBA/1J mice (8 weeks old) were obtained from Medcona and kept in a specific pathogen-free facility. The CIA model was established as previously reported (34). On the 21st day after the initial immunization, the mice were administered with an incomplete Freund (Sigma-Aldrich) 100 μg bovine type II collagen through enhanced intradermal injection. Mice were then randomly divided into five groups (n = 6): sham, CIA, MTX (1 mg/kg/3days), NOB (20 mg/kg/3days), and

ASBMB

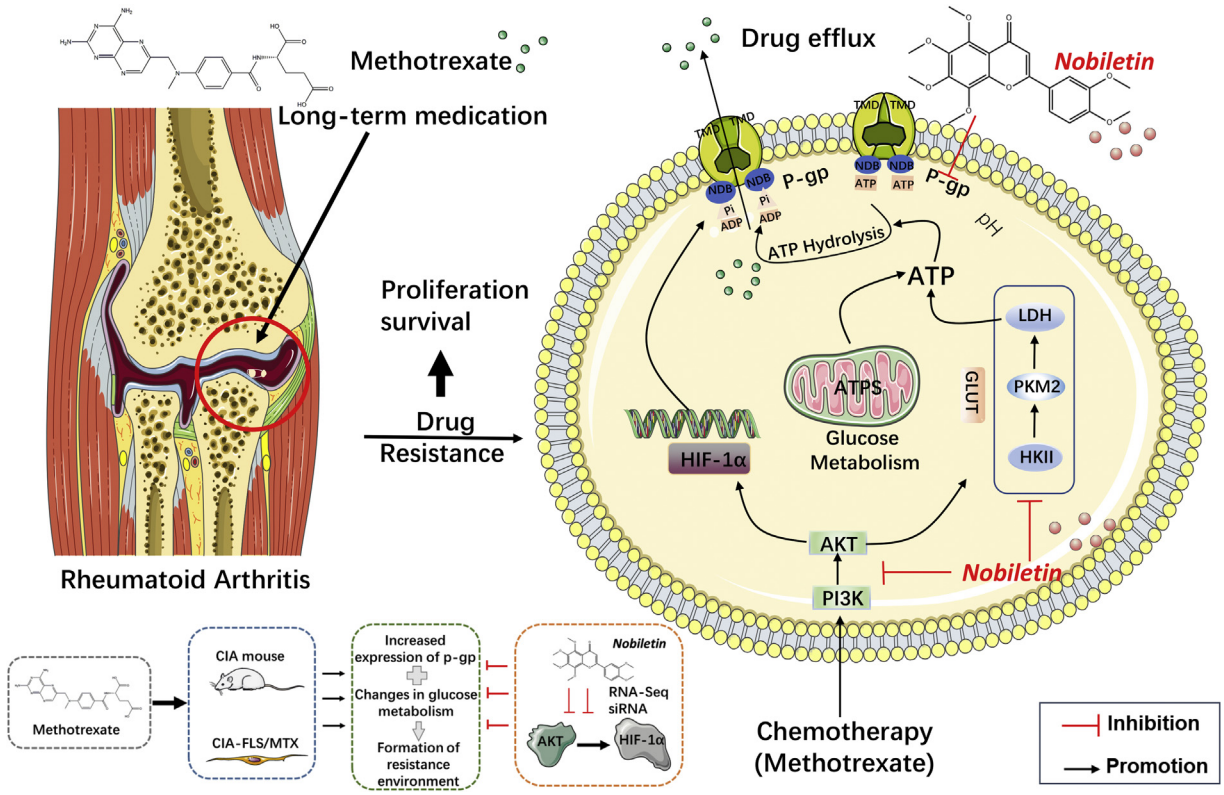

Figure 7. The mechanism through which NOB reverses MTX-induced RA resistance. Nobiletin downregulated the AKT/HIF-1α signaling pathway, thereby maintaining the drug efflux caused by the activation of P-gp. In addition, NOB significantly inhibits glycolysis and metabolic activity of CIA-FLS/MTX cells for energy and nutrition supply, thereby increasing the efficacy in response to MTX in RA. AKT, protein kinase B; CIA, collagen II-induced arthritis; HIF1-α, hypoxia-inducible factor-1 α; MTX, methotrexate; NOB, nobiletin; P-gp, P-glycoprotein; RA, rheumatoid arthritis.

MTX (1 mg/kg/3days) + NOB (20 mg/kg/3days). All the experimental mice were orally fed with the treatments from day 26 to day 64.

Evaluation of arthritis

The AI was tested every 3 days after the first immunization. The quantitative classification of arthritis severity was as follows: level 0 - no swelling; level 1 - erythema and slight swelling of the ankle joint or one-digit; level 2 - erythema and slight swelling from ankle to toe joint; level 3 - erythema and moderate swelling from the ankle joint to the metatarsophalangeal joint or palm joint; and level 4 - erythema and severe swelling from ankle to toe joint.

Analysis of micro-CT

A sample of the mice forepaw and ankle joint was selected for micro-CT (SkyScan 1176, SkyScan) scanning. The scanning parameters of micro-CT were voltage 50Kvp, micepower 40W, and six superimposed frames. After scanning and reconstruction, three-dimensional image screenshot and bone parameter analysis were performed.

Histological observation

The dissected knee joint was fixed in 10% neutral formalin buffer for 1 week. Next, the sample was embedded in paraffin, cut into 5μm-thick sections, stained with H&E, and observed under a microscope (Olympus CX23). Histopathological score evaluation criteria are as follows: according to the edema, structural changes, inflammatory cell infiltration of lesions, from light to heavy, it can be divided into 5 degrees of 0 to 4 points and finally, according to the total score calculation statistics.

Immunohistochemistry analysis

The tissue was fixed in 4% paraformaldehyde fixative solution at 4 °C and then deparaffinized. The tissues were treated with xylene and dehydrated using different concentrations of ethanol. Subsequently, it was blocked with 3% H_2O_2 and incubated with P-gp primary antibody overnight at 4 °C. The sample was dyed with DBA and hematoxylin. Finally, it was dehydrated and sealed and observed under a microscope.

Measurement of cytokine level by ELISA

Ankle joint tissue (40 mg) was washed with cold saline and homogenized in nine volumes of cold saline. The supernatant was collected and stored at −80 °C. The levels of TNF-α, IL-6, and IL-1β were measured using their corresponding ELISA kits (Uscn Life) according to the manufacturer's instructions.

Cell lines and cell culture

The CIA-FLS and CIA-FLS/MTX cell lines were purchased from the Shanghai Institute of Cell Biology in the Chinese

Academy of Sciences. They were cultured in 1640 medium containing 10% fetal bovine serum at 37 °C and 5% CO_2. Two hundred microgram/milliliter MTX was added to the CIA-FLS/MTX cells after every three generations to make the cells resistant to MTX.

Drug sensitivity assays

The viability of cells after drug treatment was explored using cell counting kit-8 assay. Briefly, the cells were seeded in a 96-well plate (at a density of 1×10^4 per well), and the cell counting kit-8 reagent was added to each well after 72 h of treatment with different concentrations of cytotoxic agents. The absorbance was recorded at 490 nm using a microplate reader (BioTek). For each group, three independent repeats were performed.

Transcriptome sequencing-based analysis

Total RNA was extracted from the cells using TRIzol reagent. The concentration of extracted RNA was determined using Nanodrop machine based on A260/280 and A260/230. RNA fragment length was measured using Agilent 2100. Sequencing libraries were prepared using NEBNext UltraTM RNA Library Preparation Kit for Illumina (NEB). The trimmed library was sequenced on the Illumina high-throughput sequencing platform (HiSeqTM2500/4000). Raw data containing some adapter contamination and low-quality reads were filtered. Other details of RNA quantification and quality analysis are provided in the supplementary material.

Quantitative RT-PCR

Total RNA was isolated from CIA-FLS and CIA-FLS/MTX cells using TRIzol reagent. The extracted RNA was reverse-transcribed to cDAN using PrimeScript RT reagent kit containing gDNA Eraser (TaKaRa, RR047). The cDNA was amplified using PCR and subjected to Realtime PCR reaction (ABI7500). For each group, three replicate wells were prepared. The primer sequences used for RT-PCR were as follows: HIF-1α: ATCTGAGGACACGAGCTGCC and GCATC GGGCTCTTTCTTAAGC; P-gp: CTTGATGGCAAAGAAAT AAAGCGAC and TGCAGTCAAACAGGATGGGCT; HK-II: GGAACCCAGCTGTTTGACCA and CAGGGGAACGAG AAGGTGAAA; PKM2: AAGTCTGGCAGGTCTGCTCAC and TCAGCACAATGACCACATCTCC; GLUT1: GATGC GGGAGAAGAAGGTCA and AGACAGCGTTGATGCCAG AC; LDH: CCGTTACCTGATGGGAGAAA and ACGTTC ACACCACTCCACAC; and β-actin: TACAACCTCCTTGC AGCTCC and GGATCTTCATGAGGTAGTCAGT. The relative mRNA level of target genes was normalized to the expression of β-actin gene.

Western blot assay

The cells and synovial tissues were treated with a radioimmunoprecipitation assay buffer containing protease inhibitors to extract proteins. The concentration of extracted proteins was determined using the bicinchoninic acid assay. The protein samples were separated on SDS-polyacrylamide gel electrophoresis and transferred into polyvinylidene fluoride membrane (Beyotime Institute of Biotechnology). The membranes were blocked with 5% skimmed milk and incubated with the following primary antibodies overnight at 4 °C: β-actin (1:1000), AKT (1:1000), p-AKT (1:1000), HIF-1α (1:1000), anti-P-gp (1:1000), HK-II (1:1000), GLUT1 (1:1000), LDH (1:1000), and PKM2 (1:1000). They were then incubated with the secondary antibody (1:5000) for 1 h at room temperature. Finally, the blots were developed using the ECL Western blot Kit (LabLead, E1050) on the Amershan Imager 600 system (GE). Image J software was used to measure the intensity of the bands.

Measurement of apoptosis using flow cytometry assay

The CIA-FLS/MTX cells were plated in 6-well plates (at a density of 2×10^4 cells per well) for 24 h and then with drugs for 24 h. The cells were digested with trypsin without EDTA and washed with 4 °C PBS buffer after treatment. They were subsequently incubated with Annexin V-FITC (559763) for 10 min, and then stained with PI for 5 min. The state of apoptosis was analyzed using flow cytometry

P-glycoprotein substrate efflux assay

To determine whether NOB can influence the function of p-gp, flow cytometry assay was adopted to measured efflux effects. Briefly, the cells were incubated with R123 (0.5 μg/ml) with or without NOB (80 μM) for 1 h. The cells were then washed twice with PBS at 4 °C, incubated without Rh123 medium for 30 min at 37 °C, and washed twice with PBS. Finally, the fluorescent intensity of Rh-123 was determined using flow cytometry assay. PSC-833 (20 μM) was used as a positive control.

Measurement of ATP level, glucose consumption, and lactate production

The CIA-FLS and CIA-FLS/MTX cells were plated in six-well plates (at a density of 2×10^4 cells per well). After 48 h of treatment with different drugs, the generation of ATP, glucose uptake, and lactate production were measured using ATP Assay Kit (A05911) , Glucose Assay Kit (361510), and Lactate Assay Kit (A01921) following the protocols provided by the manufacturer. The absorbance of each group was recorded immediately after treatment at the corresponding wavelengths using a multifunctional microplate reader (Molecular Devices).

RNAi-mediated silencing of HIF-1α and AKT

The CIA-FLS/MTX cells were seeded in 6-well plates (at a density of 1×10^5 cells per well) for 24 h. They were then transfected with siRNA (AKT1 siRNA (25 nM), HIF-1 siRNA (25 nM), or siRNA (25 nM scrambled (negative control)) reagents and Lipofectamine containing Opti-MEM. The transfection was conducted in line with the manufacturer's instructions. The protein expression of HIF-1α and AKT was measured by Western blotting assay after 48 h of transfection.

Statistical analysis

Data were analyzed using GraphPad Prism software (version 7.00, USA) and expressed as means ± SD of at least three independent experiments. For each treatment, differences between groups were compared using one-way ANOVA. * $p < 0.05$, ** $p < 0.01$, and *** $p < 0.001$ were considered as statistically significant.

Compliance with ethics requirements

The animal use protocol listed below has been reviewed and approved by the Animal Ethical and Welfare Committee (AEWC) (Approval No. MDKN-2021–002).

Data availability

Data is contained within the article.

Supporting information—This article contains supporting information.

Acknowledgments—This work was supported by Beijing Natural Science Foundation (7202111), National Science and Technology Major Project (2018ZX10101001–005–003), the Fundamental Research Funds for the Central public welfare research institutes (Z0653/Z0656), and Innovation Team and Talents Cultivation Program of National Administration of Traditional Chinese Medicine (No: ZYYCXTD-D-202005). All special thanks for the long-term subsidy mechanism from the Ministry of Finance and the Ministry of Education of PRC for BUCM.

Author contributions—Data analysis: Dongjie Zhu, Zhiwen Cao. R. L., A. L., Cheng Lu, and Y. L. methodology; R. L., Y. S., Chenxi Li, Z. Z., Z. X., Q. H., and L. Y. investigation; R. L. and Y. L. writing–original draft; R. L. and Y. L. writing–review and editing.

Conflict of interest—The authors declare that they have no conflict of interest with the contents of this article.

Abbreviations—The abbreviations used are: AI, arthritis index; AKT, protein kinase B; CIA, collagen II-induced arthritis; CIA-FLS, fibroblast-like synoviocytes from collagen-induced arthritis; CIA-FLS/MTX, MTX-resistant fibroblast-like synoviocytes from collagen-induced arthritis; DEGs, differentially expressed genes; FLS, fibroblast-like synovial cells; GLUT1, glucose transporter 1; HIF1-α, hypoxia-inducible factor-1 α; HK-II, hexokinase-II; IL, interleukin; LDH, lactic dehydrogenase; MDR, multidrug resistance; MTX, methotrexate; NOB, nobiletin; P-gp, P-glycoprotein; PKM2, pyruvate kinase isozyme type M2; RA, rheumatoid arthritis; TNF-α, tumor necrosis factor-alpha.

References

1. Takase-Minegishi, K., Horita, N., Kobayashi, K., Yoshimi, R., Kirino, Y., Ohno, S., Kaneko, T., Nakajima, H., Wakefield, R. J., and Emery, P. (2018) Diagnostic test accuracy of ultrasound for synovitis in rheumatoid arthritis: Systematic review and meta-analysis. *Rheumatology* **57**, 49–58
2. Groff, G. D., Shenberger, K. N., Wilke, W. S., and Taylor, T. H. (1983) Low dose oral methotrexate in rheumatoid arthritis: An uncontrolled trial and review of the literature. *Semin. Arthritis Rheum.* **12**, 333–347
3. Calabrese, L. H., Calabrese, C., and Kirchner, E. (2016) The 2015 American College of Rheumatology Guideline for the Treatment of Rheumatoid Arthritis Should Include New Standards for Hepatitis B Screening: Comment on the Article by Singh et al. *Arthritis Care Res.* **68**, 723–724
4. Gifford, A. J., Kavallaris, M., Madafiglio, J., Matherly, L. H., Stewart, B. W., Haber, M., and Norris, M. D. (1998) P-glycoprotein-mediated methotrexate resistance in CCRF-CEM sublines deficient in methotrexate accumulation due to a point mutation in the reduced folate carrier gene. *Int. J. Cancer* **78**, 176–181
5. Dong, C., Chen, Y., Ma, J., Yang, R., Li, H., Liu, R., You, D., Luo, C., Li, H., Yang, S., Ke, K., Lin, M. C., and Chen, C. (2020) Econazole nitrate reversed the resistance of breast cancer cells to adriamycin through inhibiting the PI3K/AKT signaling pathway. *Am. J. Cancer Res.* **10**, 263–274
6. Briz, O., Perez-Silva, L., Al-Abdulla, R., Abete, L., Reviejo, M., Romero, M. R., and Marin, J. J. G. (2019) What "The Cancer Genome Atlas" database tells us about the role of ATP-binding cassette (ABC) proteins in chemoresistance to anticancer drugs. *Expert Opin. Drug Metab. Toxicol.* **15**, 577–593
7. Norris, M. D., De Graaf, D., Haber, M., Kavallaris, M., Madafiglio, J., Gilbert, J., Kwan, E., Stewart, B. W., Mechetner, E. B., Gudkov, A. V., and Roninson, I. B. (1996) Involvement of MDR1 P-glycoprotein in multifactorial resistance to methotrexate. *Int. J. Cancer* **65**, 613–619
8. Xu, S. W., Law, B. Y. K., Qu, S. L. Q., Hamdoun, S., Chen, J., Zhang, W., Guo, J. R., Wu, A. G., Mok, S. W. F., Zhang, D. W., Xia, C., Sugimoto, Y., Efferth, T., Liu, L., and Wong, V. K. W. (2020) SERCA and P-glycoprotein inhibition and ATP depletion are necessary for celastrol-induced autophagic cell death and collateral sensitivity in multidrug-resistant tumor cells. *Pharmacol. Res.* **153**, 104660
9. Marki-Zay, J., Tauberne Jakab, K., Szeremy, P., and Krajcsi, P. (2013) MDR-ABC transporters: Biomarkers in rheumatoid arthritis. *Clin. Exp. Rheumatol.* **31**, 779–787
10. Jeevitha Priya, M., Vidyalakshmi, S., and Rajeswari, M. (2020) Study on reversal of ABCB1 mediated multidrug resistance in Colon cancer by acetogenins: An in-silico approach. *J. Biomol. Struct. Dyn.* https://doi.org/10.1080/07391102.2020.1855249
11. Tsujimura, S., Adachi, T., Saito, K., Kawabe, A., and Tanaka, Y. (2018) Relevance of P-glycoprotein on CXCR4(+) B cells to organ manifestation in highly active rheumatoid arthritis. *Mod. Rheumatol.* **28**, 276–286
12. Huang, H., Li, L., Shi, W., Liu, H., Yang, J., Yuan, X., and Wu, L. (2016) The multifunctional effects of nobiletin and its metabolites *in vivo* and *in vitro*. *Evid Based. Complement. Alternat. Med.* **2016**, 2918796
13. Feng, S., Zhou, H., Wu, D., Zheng, D., Qu, B., Liu, R., Zhang, C., Li, Z., Xie, Y., and Luo, H. B. (2020) Nobiletin and its derivatives overcome multidrug resistance (MDR) in cancer: Total synthesis and discovery of potent MDR reversal agents. *Acta Pharm. Sin. B* **10**, 327–343
14. Ashrafizadeh, M., Zarrabi, A., Saberifar, S., Hashemi, F., Hushmandi, K., Hashemi, F., Moghadam, E. R., Mohammadinejad, R., Najafi, M., and Garg, M. (2020) Nobiletin in cancer therapy: How this plant derived-natural compound targets various oncogene and onco-Suppressor pathways. *Biomedicines* **8**, 110
15. Lee, J. H., Kim, C., Um, J. Y., Sethi, G., and Ahn, K. S. (2019) Casticin-induced inhibition of cell growth and survival are mediated through the dual modulation of Akt/mTOR signaling cascade. *Cancers (Basel)* **11**, 254
16. He, D., Liu, Z., Wang, M., Shu, Y., Zhao, S., Song, Z., Li, H., Liu, L., Liang, W., Li, W., Cao, Z., Lu, C., Lu, A., and Liu, Y. (2019) Synergistic enhancement and hepatoprotective effect of combination of total phenolic extracts of citrus aurantium L. and methotrexate for treatment of rheumatoid arthritis. *Phytotherapy Res.* **33**, 1122–1133
17. Liu, Z., Guo, S., and Dong, Q. (2020) Nobiletin suppresses IL-21/IL-21 receptor-mediated inflammatory response in MH7A fibroblast-like synoviocytes (FLS): An implication in rheumatoid arthritis. *Eur. J. Pharmacol.* **875**, 172939
18. Kaihara, K., Nakagawa, S., Arai, Y., Inoue, H., Tsuchida, S., Fujii, Y., Kamada, Y., Kishida, T., Mazda, O., and Takahashi, K. (2021) Sustained hypoxia suppresses joint destruction in a rat model of rheumatoid

arthritis *via* negative feedback of hypoxia inducible factor-1alpha. *Int. J. Mol. Sci.* **22**, 3898
19. McGarry, T., Orr, C., Wade, S., Biniecka, M., Wade, S., Gallagher, L., Low, C., Veale, D. J., and Fearon, U. (2018) JAK/STAT blockade alters synovial bioenergetics, mitochondrial function, and proinflammatory mediators in rheumatoid arthritis. *Arthritis Rheumatol.* **70**, 1959–1970
20. Li, G. Q., Zhang, Y., Liu, D., Qian, Y. Y., Zhang, H., Guo, S. Y., Sunagawa, M., Hisamitsu, T., and Liu, Y. Q. (2013) PI3 kinase/Akt/HIF-1alpha pathway is associated with hypoxia-induced epithelial-mesenchymal transition in fibroblast-like synoviocytes of rheumatoid arthritis. *Mol. Cell Biochem.* **372**, 221–231
21. Hua, S., and Dias, T. H. (2016) Hypoxia-inducible factor (HIF) as a target for novel therapies in rheumatoid arthritis. *Front. Pharmacol.* **7**, 184
22. Wang, T., Jiao, Y., and Zhang, X. (2021) Immunometabolic pathways and its therapeutic implication in autoimmune diseases. *Clin. Rev. Allergy Immunol.* **60**, 55–67
23. Fletcher, J. I., Williams, R. T., Henderson, M. J., Norris, M. D., and Haber, M. (2016) ABC transporters as mediators of drug resistance and contributors to cancer cell biology. *Drug Resist. updat.* **26**, 1–9
24. de Oliveira, P. G., Farinon, M., Sanchez-Lopez, E., Miyamoto, S., and Guma, M. (2019) Fibroblast-like synoviocytes glucose metabolism as a therapeutic target in rheumatoid arthritis. *Front. Immunol.* **10**, 1743
25. Storelli, F., Anoshchenko, O., and Unadkat, J. D. (2021) Successful prediction of human steady-state unbound brain-to-plasma concentration ratio of P-gp substrates using the proteomics-informed relative expression factor approach. *Clin. Pharmacol. Ther.* **110**, 432–442
26. Muhammad, I. I., Kong, S. L., Akmar Abdullah, S. N., and Munusamy, U. (2019) RNA-seq and ChIP-seq as complementary approaches for comprehension of plant transcriptional regulatory mechanism. *Int. J. Mol. Sci.* **21**, 167
27. Chen, J., Cheng, W., Li, J., Wang, Y., Chen, J., Shen, X., Su, A., Gan, D., Ke, L., Liu, G., Lin, J., Li, L., Bai, X., and Zhang, P. (2021) Notch-1 and Notch-3 mediates hypoxia-induced synovial fibroblasts activation in rheumatoid arthritis. *Arthritis Rheumatol.* **73**, 1810–1819
28. Tripathi, S. C., Fahrmann, J. F., Celiktas, M., Aguilar, M., Marini, K. D., Jolly, M. K., Katayama, H., Wang, H., Murage, E. N., Dennison, J. B., Watkins, D. N., Levine, H., Ostrin, E. J., Taguchi, A., and Hanash, S. M. (2017) MCAM mediates chemoresistance in Small-cell lung cancer *via* the PI3K/AKT/SOX2 signaling pathway. *Cancer Res.* **77**, 4414–4425
29. Long, Q. Z., Zhou, M., Liu, X. G., Du, Y. F., Fan, J. H., Li, X., and He, D. L. (2013) Interaction of CCN1 with alphavbeta3 integrin induces P-glycoprotein and confers vinblastine resistance in renal cell carcinoma cells. *Anticancer Drugs* **24**, 810–817
30. Alexa-Stratulat, T., Pesic, M., Gasparovic, A. C., Trougakos, I. P., and Riganti, C. (2019) What sustains the multidrug resistance phenotype beyond ABC efflux transporters? Looking beyond the tip of the iceberg. *Drug Resist. Updat.* **46**, 100643
31. Masoumi, M., Mehrabzadeh, M., Mahmoudzehi, S., Mousavi, M. J., Jamalzehi, S., Sahebkar, A., and Karami, J. (2020) Role of glucose metabolism in aggressive phenotype of fibroblast-like synoviocytes: Latest evidence and therapeutic approaches in rheumatoid arthritis. *Int. Immunopharmacol.* **89**, 107064
32. Zhang, Z., Tan, X., Luo, J., Yao, H., Si, Z., and Tong, J. S. (2020) The miR-30a-5p/CLCF1 axis regulates sorafenib resistance and aerobic glycolysis in hepatocellular carcinoma. *Cell Death Dis.* **11**, 902
33. Asgari, Y., Zabihinpour, Z., Salehzadeh-Yazdi, A., Schreiber, F., and Masoudi-Nejad, A. (2015) Alterations in cancer cell metabolism: The warburg effect and metabolic adaptation. *Genomics* **105**, 275–281
34. Miyoshi, M., and Liu, S. (2018) Collagen-induced arthritis models. *Methods Mol. Biol.* **1868**, 3–7